Supplementary Information

Exploring magnetic anisotropy and exchange coupling in $Fe^{III}_2Dy^{III}$ heterotrimetallic assemblies displaying slow relaxation of magnetization

Anangamohan Panja,*[a,b] Zvonko Jagličić,[c] Narayan Ch. Jana,[b] Scarlette Contesso,[d] Paula Brandão,[e] Daniel Aravena[d]

[a] *Department of Chemistry, Gokhale Memorial Girls' College, 1/1 Harish Mukherjee Road, Kolkata-700020, India. E-mail: ampanja@yahoo.co.in*

[b] *Department of Chemistry, Panskura Banamali College, Panskura RS, WB 721152, India*

[c] *Institute of Mathematics, Physics and Mechanics & Faculty of Civil and Geodetic Engineering, University of Ljubljana, Jadranska 19, 1000 Ljubljana, Slovenia*

[d] *Department of Materials Chemistry, Faculty of Chemistry and Biology, University of Santiago de Chile, Casilla 40, Correo 33, Santiago, Chile*

[e] *Department of Chemistry, CICECO-Aveiro Institute of Materials, University of Aveiro, 3810-193 Aveiro, Portugal*

Table S1. Crystal data and structure refinement for Ligand HL^3 and complexes **1-3**.

	HL^3	**1**	**2**	**3**
Empirical formula	$C_{15}H_{14}ClNO_2$	$C_{60}H_{60}DyFe_2N_5O_{19}$	$C_{76}H_{104}DyFe_2N_5O_{25}$	$C_{66}H_{65}Cl_5DyFe_2N_4O_{18.5}$
Formula weight	275.72	1429.33	1761.84	1661.67
Temperature/K	100.15	150.15	150.15	150.00
Crystal system	orthorhombic	monoclinic	monoclinic	triclinic
Space group	*P*bca	I2/a	$P2_1/c$	P-1
a/Å	6.5726(3)	17.9305(6)	16.6187(5)	15.5272(16)
b/Å	16.3198(9)	12.5854(3)	27.2829(8)	18.8507(19)
c/Å	24.6147(13)	25.8640(7)	18.6130(5)	25.889(3)
α/°	90	90	90	99.325(4)
β/°	90	104.547(3)	105.229(3)	91.237(4)
γ/°	90	90	90	106.046(4)
Volume/Å^3	2640.3(2)	5649.4(3)	8142.9(4)	7168.5(13)
Z	8	4	4	4
ρ_{calc}g/cm^3	1.387	1.680	1.437	1.540
μ/mm^{-1}	0.286	11.737	1.338	1.688
F(000)	1152.0	2900.0	3652.0	3360.0
Radiation	MoKα (λ = 0.71073)	CuKα (λ = 1.54184)	MoKα (λ = 0.71073)	MoKα (λ = 0.71073)
2Θ range for data collection/°	4.992 to 61.104	7.062 to 156.51	3.75 to 61.304	4.03 to 54.414
Reflections collected	16961	23073	94521	32276
Independent reflections	3307 [R_{int} = 0.0450, R_{sigma} = 0.0379]	5850 [R_{int} = 0.0515, R_{sigma} = 0.0412]	20308 [R_{int} = 0.0751, R_{sigma} = 0.0666]	32276 [R_{int} = ?, R_{sigma} = 0.0387]
Data/restraints/parameters	3307/0/175	5850/83/441	20308/132/972	32276/183/1856
Goodness-of-fit on F^2	1.040	1.012	1.033	1.101
Final R indexes [I>=2σ (I)]	R_1 = 0.0354, wR_2 = 0.0837	R_1 = 0.0338, wR_2 = 0.0784	R_1 = 0.0431, wR_2 = 0.0987	R_1 = 0.0434, wR_2 = 0.1002
Final R indexes [all data]	R_1 = 0.0490, wR_2 = 0.0899	R_1 = 0.0410, wR_2 = 0.0821	R_1 = 0.0660, wR_2 = 0.1096	R_1 = 0.0617, wR_2 = 0.1150
Largest diff. peak/hole / e Å^{-3}	0.38/-0.20	0.56/-0.73	1.21/-1.02	1.35/-2.44

Table S2. Selected bond distances (in Å) around the Fe^{III} centers in complexes **1-3**.

1		**2**		**3**			
Fe1–O1	2.025(2)	Fe1–O3	2.052(2)	Fe1A–O1A	2.036(3)	Fe1B–O1B	2.034(3)
Fe1–O6	2.059(2)	Fe1–O1	1.914(2)	Fe1A–O3A	1.884(3)	Fe1B–O3B	1.899(3)
Fe1–O4	1.941(2)	Fe1–O4	2.042(2)	Fe1A–O9A	2.022(3)	Fe1B–O9B	2.037(3)
Fe1–O3	1.952(2)	Fe1–O6	1.933(2)	Fe1A–O13A	1.965(3)	Fe1B–O13B	1.954(3)
Fe1– N2	2.164(2)	Fe1–N1	2.171(3)	Fe1A–N1A	2.213(4)	Fe1B–N1B	2.182(4)
Fe1–N1	2.186(2)	Fe1–N2	2.204(3)	Fe1A–N2A	2.166(4)	Fe1B–N2B	2.200(4)
		Fe2–O10	2.004(2)	Fe2A–O5A	2.048(3)	Fe2B–O5B	1.999(3)
		Fe2–O7	1.922(2)	Fe2A–O7A	1.894(3)	Fe2B–O7B	1.875(3)
		Fe2–O9	2.069(2)	Fe2A–O11A	2.040(3)	Fe2B–O11B	2.025(3)
		Fe2–O12	1.949(2)	Fe2A–O14A	1.946(3)	Fe2B–O14B	1.967(3)
		Fe2–N4	2.182(3)	Fe2A–N3A	2.185(4)	Fe2B–N3B	2.217(4)
		Fe2–N3	2.124(3)	Fe2A–N4A	2.194(4)	Fe2B–N4B	2.172(4)

Table S3. Selected bond distances around the Dy^{III} centers in complexes **1-3**.

1		**2**		**3**[#]			
Dy1–O1	2.325(2)	Dy1–O10	2.302(2)	DyA–O1A	2.331(3)	DyB–O1B	2.341(3)
Dy1–O1[1]	2.325(2)	Dy1–O9	2.337(2)	DyA–O2A	2.557(3)	DyB–O2B	2.580(3)
Dy1–O6[1]	2.349(2)	Dy1–O3	2.359(2)	DyA–O5A	2.337(3)	DyB–O5B	2.334(3)
Dy1–O6	2.349(2)	Dy1–O5	2.666(2)	DyA–O6A	2.560(3)	DyB–O6B	2.531(3)
Dy1–O2[1]	2.682(2)	Dy1–O4	2.286(2)	DyA–O10A	2.296(3)	DyB–O10B	2.296(3)
Dy1–O2	2.682(2)	Dy1–O11	2.890(2)	DyA–O12A	2.310(3)	DyB–O12B	2.305(3)
Dy1–O7[1]	2.377(2)	Dy1–O13	2.324(2)	DyA–O13A	2.288(3)	DyB–O13B	2.309(3)
Dy1–O7	2.377(2)	Dy1–O15	2.408(2)	DyA–O14A	2.290(3)	DyB–O14B	2.287(3)
Dy1–O8	2.457(3)	Dy1–O14	2.426(2)				
Dy1–O8[1]	2.457(3)						

[1]Symmetry code = 1/2-X,+Y,1-Z; [#] A and B denote crystallographically distinguishable complex cations

Table S4. Shape analysis around the Fe^{III} centers in complexes **1-3**.

Label	Shape	Symmetry	**1**	**2**		**3**	
			Fe1	Fe1	Fe2	Fe1A	Fe2A
HP-6	Hexagon	D_{6h}	32.110	31.150	31.150	32.957	32.557
PPY-6	Pentagonal pyramid	C_{5v}	11.177	15.148	15.148	24.003	24.274
OC-6	Octahedron	Oh	13.954	7.131	7.131	**1.335**	**1.292**
TPR-6	Trigonal prism	D_{3h}	**1.292**	**3.374**	**3.374**	11.455	11.652
JPPY-6	Johnson pentagonal pyramid J2	C_{5v}	14.456	18.550	18.550	28.270	28.028

Table S5. Shape analysis around the Dy^{III} centers in complexes **1** and **2.**

Label	Shape	Symmetry	**1**	**2**
EP-9	Enneagon	D_{9h}	34.200	34.093
OPY-9	Octagonal pyramid	C_{8v}	23.235	24.124
HBPY-9	Heptagonal bipyramid	D_{7h}	14.544	15.724
JTC-9	Johnson triangular cupola J3	C_{3v}	14.903	15.238
JCCU-9	Capped cube J8	C_{4v}	7.457	8.256
CCU-9	Spherical-relaxed capped cube	C_{4v}	6.951	7.690
JCSAPR-9	Capped square antiprism J10	C_{4v}	3.283	3.526
CSAPR-9	**Spherical capped square antiprism**	**C_{4v}**	**3.088**	**3.210**
JTCTPR-9	**Tricapped trigonal prism J51**	**D_{3h}**	**2.846**	**2.753**
TCTPR-9	**Spherical tricapped trigonal prism**	**D_{3h}**	**2.706**	**2.895**
JTDIC-9	Tridiminishd icosahedron J63	C_{3v}	11.440	10.895
HH-9	Hula-hoop	C_{2v}	8.645	9.225
MFF-9	**Muffin**	**C_s**	**2.899**	3.545

Table S6. Shape analysis around the Dy^{III} centers in complexes **3**.

Label	**Shape**	**Symmetry**	**3**	
			DyA	**DyB**
OP-8	Octagon	D_{8h}	32.676	32.460
HPY-8	Heptagonal pyramid	C_{7v}	20.914	20.336
HBPY-8	Hexagonal bipyramid	D_{6h}	13.129	11.739
CU-8	Cube	Oh	9.612	7.868
SAPR-8	**Square antiprism**	**D_{4d}**	**1.319**	**1.427**
TDD-8	Triangular dodecahedron	D_{2d}	2.747	2.714
JGBF-8	Johnson gyrobifastigium J26	D_{2d}	12.639	12.736
JETBPY-8	Johnson elongated triangular bipyramid J14	D_{3h}	29.010	28.766
JBTPR-8	Biaugmented trigonal prism J50	C_{2v}	2.996	3.405
BTPR-8	Biaugmented trigonal prism	C_{2v}	2.660	3.149
JSD-8	Snub diphenoid J84	D_{2d}	4.737	5.618
TT-8	Triakis tetrahedron	Td	10.445	8.710
ETBPY-8	Elongated trigonal bipyramid	D_{3h}	23.447	23.481

Table S7. CASSCF(9,7) calculated g-factors and energies for the Kramers' doublets of the ground $^6H_{15/2}$ multiplet for **1**-**3**.

Complex	**E (cm^{-1})**	**g_x**	**g_y**	**g_z**
1	0.0	0.048	0.082	19.619
	86.5	0.316	0.341	16.770
	198.5	1.556	3.354	11.981
	241.8	0.201	5.248	10.196
	264.5	1.113	2.236	15.525
	326.8	2.353	5.164	10.972
	428.3	0.107	1.916	13.803
	484.0	0.667	2.868	16.826
2	0.0	0.035	0.069	19.564
	101.5	0.367	0.553	16.420
	181.2	0.922	1.513	13.198
	258.3	2.648	3.013	12.106
	309.8	0.822	3.170	11.215
	376.1	7.096	9.291	4.074
	508.4	0.732	1.069	15.934
	608.6	0.209	0.612	18.659
3a	0	0.130	0.418	18.454
	74.9	0.162	0.358	19.188

	88.3	0.836	1.411	14.534
	139.4	2.205	3.668	14.343
	192.0	3.610	6.637	9.721
	318.3	1.852	4.549	11.509
	381.4	1.195	4.291	12.768
	452.0	0.470	1.845	17.469
3b	0.0	0.121	0.380	18.481
	93.3	0.838	4.763	11.682
	100.8	0.408	3.322	14.141
	173.0	2.905	4.677	10.292
	196.2	1.641	3.400	13.492
	323.6	2.501	4.441	10.501
	408.0	4.503	6.061	1.685
	460.1	8.211	12.187	1.096

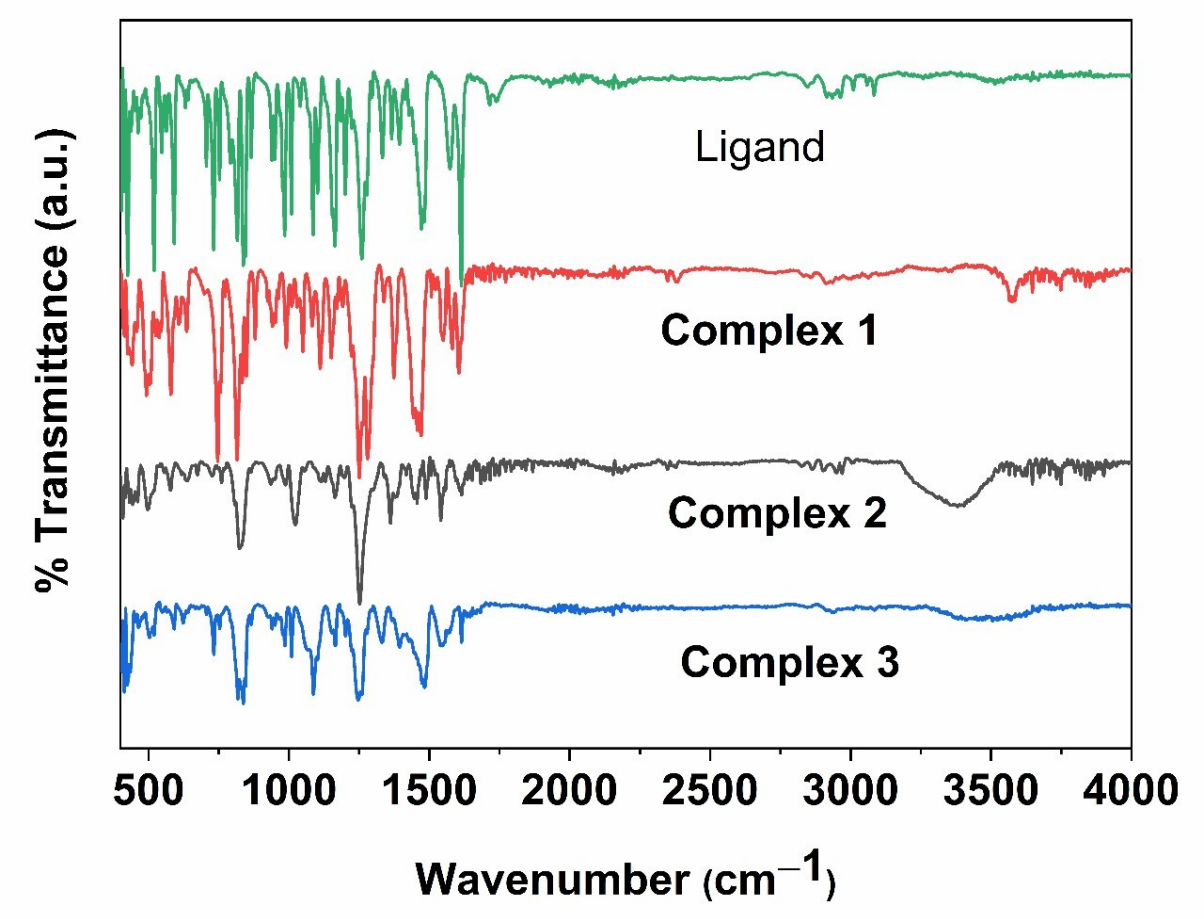

Fig. S1. IR spectra of ligand HL^3 and complexes **1**−**3**.

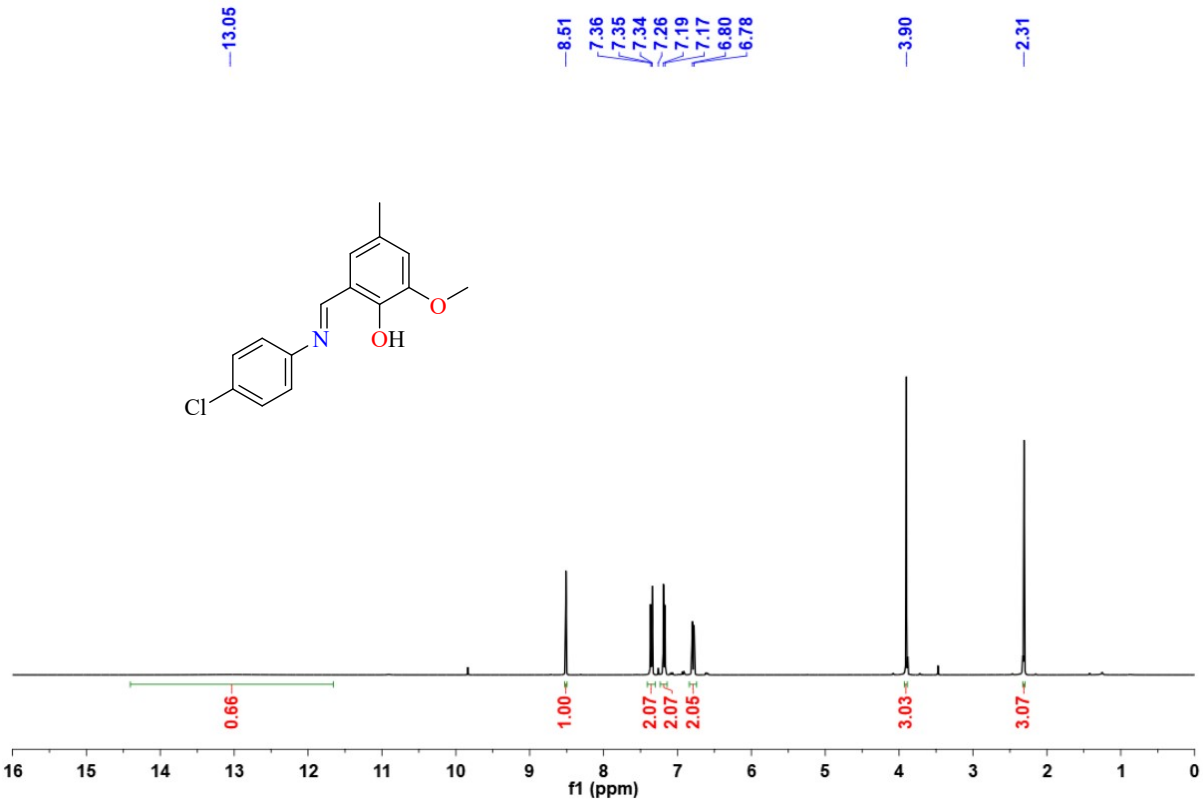

Fig. S2. ^{1}H NMR spectra of the ligand HL^{3} in $CDCl_3$ at room temperature.

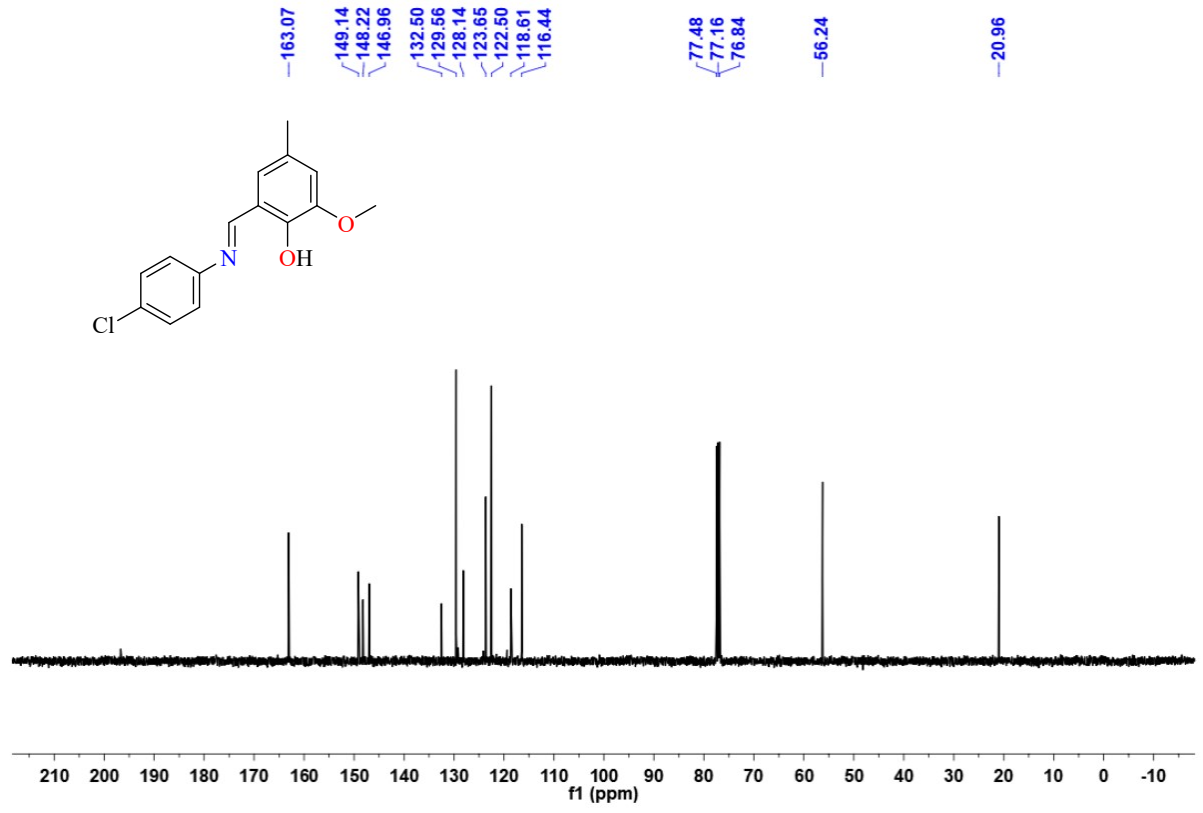

Fig. S3. ^{13}C NMR spectra of the ligand HL^{3} in $CDCl_3$ at room temperature.

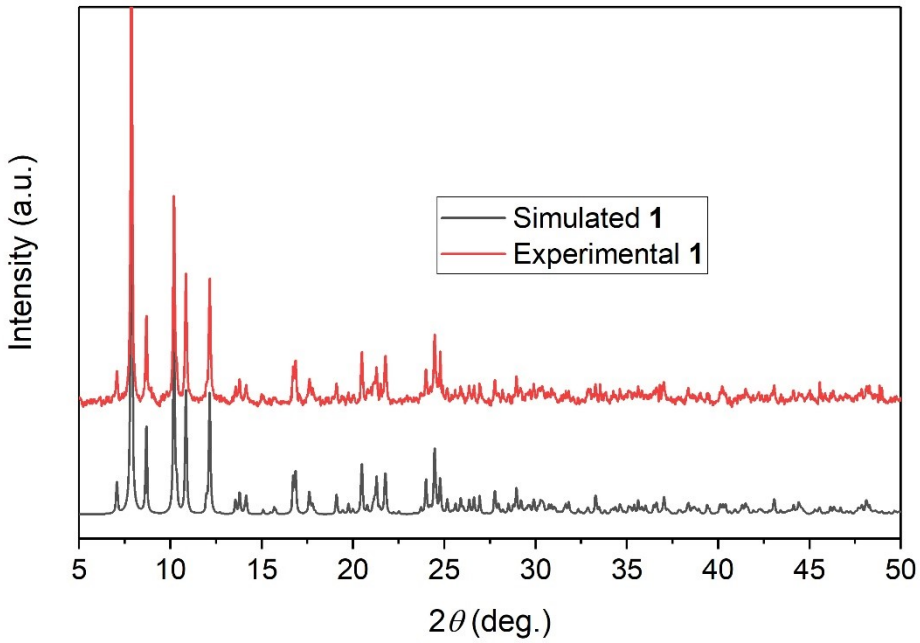

Fig. S4. PXRD data for complex **1**.

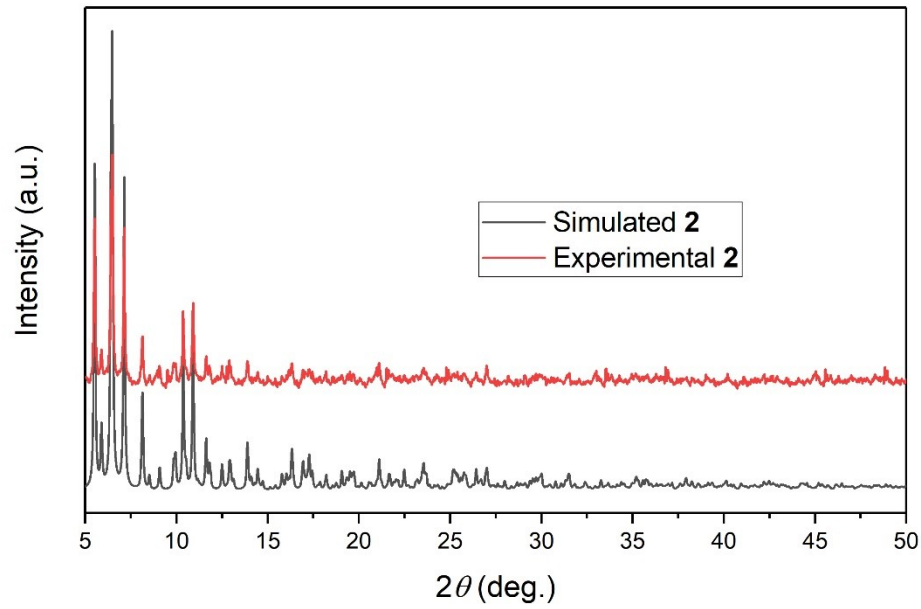

Fig. S5. PXRD data for complex **2**.

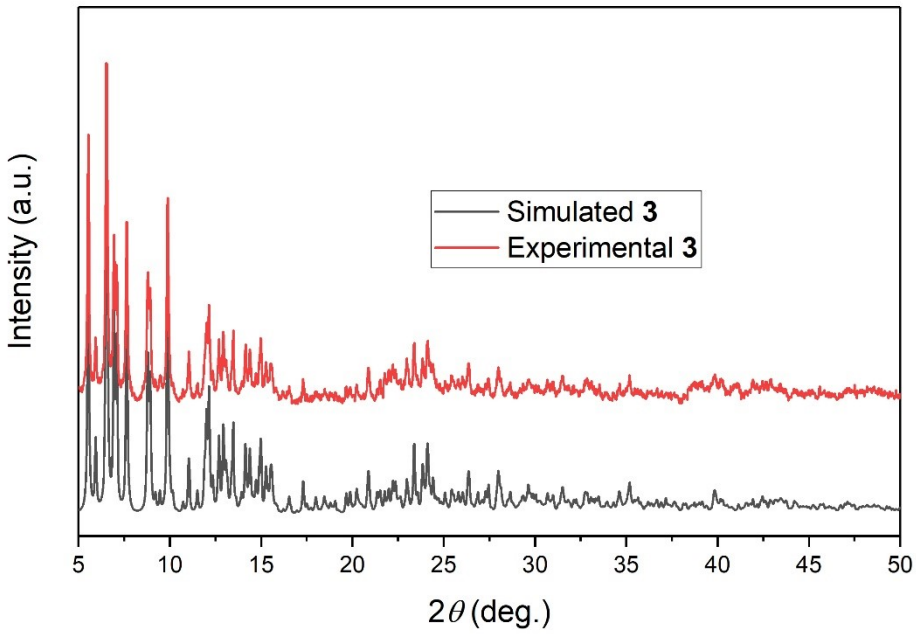

Fig. S6. PXRD data for complex **3**.

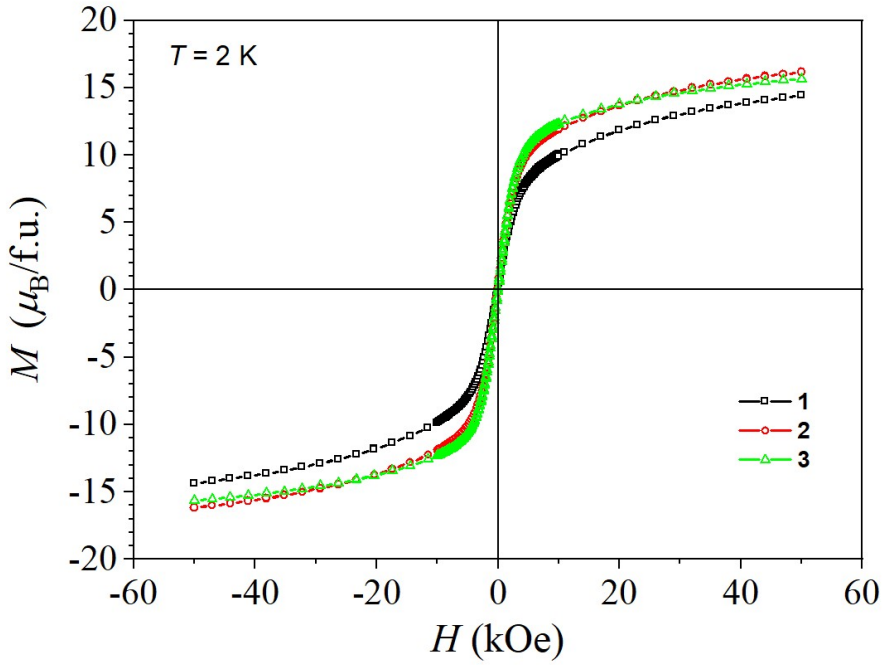

Fig. S7. Magnetization plots of **1**−**3** at 2 K.

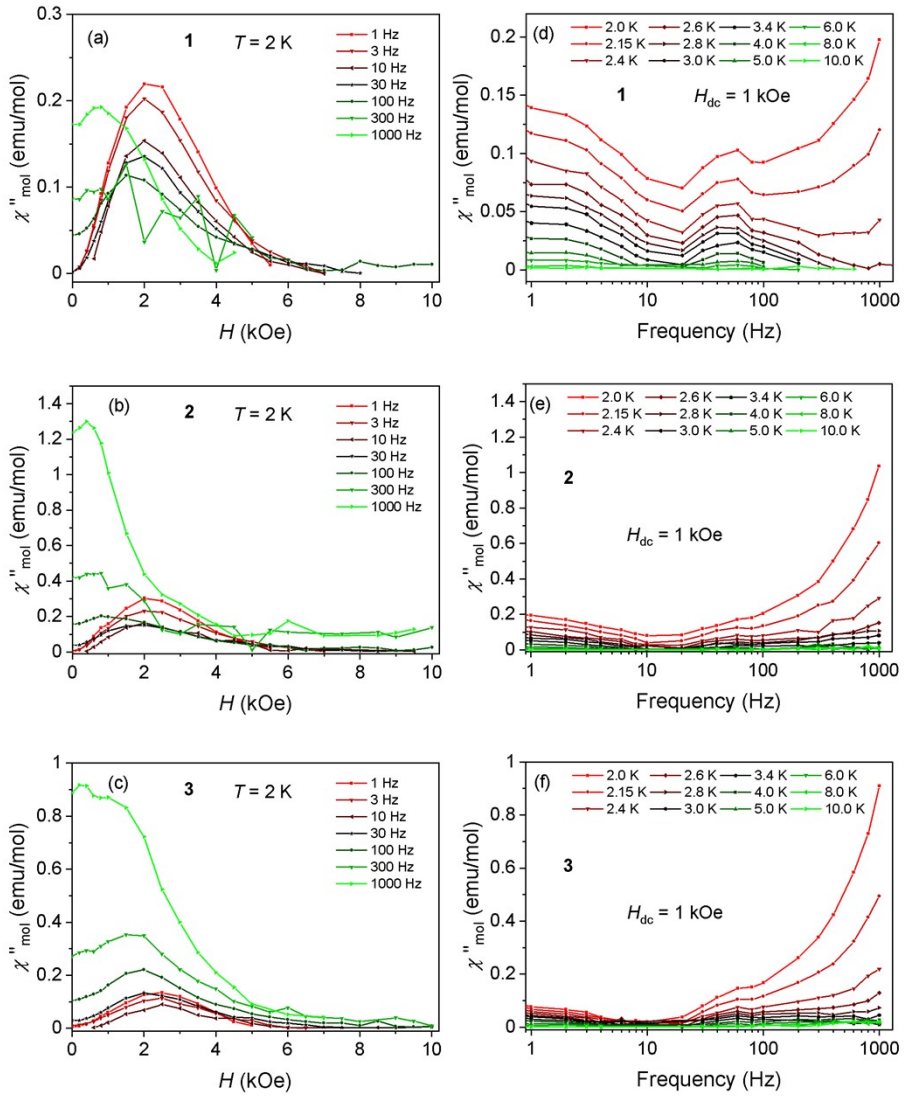

Fig. S8. Field-dependent χ″ plots for complexes **1–3** at 2 K (left), and frequency-dependent χ″ plots at 1.0 kOe applied DC field (right).

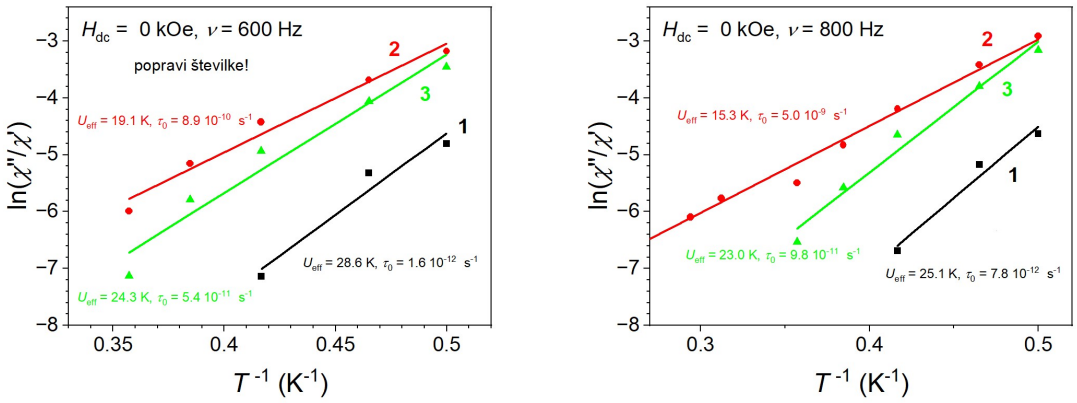

Fig. S9. Plot of ln(χ''/χ') versus T^{-1} at 600 Hz and 800 Hz under zero field for complexes **1–3**. The relaxation times and effective energy barriers were obtained from linear fitting in the temperature range below 4 K using the equation described in the text.